

**ACUCARE: INTEGRATING IMAGE PROCESSING AND FEATURE-  
BASED LEARNING INTO A MOBILE APP FOR ACNE DETECTION  
AND CLASSIFICATION**



By

Zuha Fatima

Humna Ali

Supervisors

Mr. Tufail Shah

Ms. Ifrah Mansoor

Department of Computing

Institute of Space Technology, Islamabad

2025

**ACUCARE: INTEGRATING IMAGE PROCESSING AND FEATURE-  
BASED LEARNING INTO A MOBILE APP FOR ACNE DETECTION  
AND CLASSIFICATION**

A thesis submitted to the  
Institute of Space Technology  
in partial fulfillment of the requirements  
for the degree of Bachelor of Science in  
Computer Science

By  
Zuha Fatima  
Humna Ali

Supervisors  
Mr. Tufail Shah  
Ms. Ifrah Mansoor

Department of Computing  
Institute of Space Technology, Islamabad  
2025

Department of Computing  
Institute of Space Technology, Islamabad

Institute of Space Technology, Islamabad

Department of Computing



**ACUCARE: INTEGRATING IMAGE PROCESSING AND FEATURE-  
BASED LEARNING INTO A MOBILE APP FOR ACNE DETECTION  
AND CLASSIFICATION**

By

Zuha Fatima

Humna Ali

**APPROVAL BY BOARD OF EXAMINERS**

---

Supervisor

---

Co-Supervisor

---

Internal Examiner

---

External Examiner

## **CERTIFICATE**

This is to certify that the research work described in this thesis is the original work of the author and has been carried out under my direct supervision. I have personally gone through all the data/results/materials reported in the manuscript and certify their correctness/authenticity. I further certify that the material included in this thesis is not plagiarized and has not been used in part or full in a manuscript already submitted or in the process of submission in partial/complete fulfillment of the award of any other degree from any institution. I also certify that the thesis has been prepared under my supervision according to the prescribed format and I endorse its evaluation for the award of Bachelor of Science in Electrical Engineering degree through the official procedures of the Institute.

---

## **AUTHORS DECLARATION**

We take full responsibility of the research work conducted during the thesis titled **“AcuCare: Integrating image processing and feature-based learning into a mobile app for acne detection and classification”**.

We solemnly declare that the research and development work presented in the thesis is done solemnly by us with no significant help from any other person; however, small help wherever taken is duly acknowledged. We have also written the thesis by ourselves. Moreover, we have not presented this thesis or any part of the thesis previously to any other degree awarding institution within Pakistan or abroad.

we understand that the management of IST has a zero-tolerance policy towards plagiarism. Therefore, we as authors of the above mentioned thesis solemnly declare that no portion of my thesis has been plagiarized and any material used in this Thesis does not contain any literal citing (verbatim) of more than 70 words (total) even by giving a reference unless we have obtained the written permission of the publisher to do so. Furthermore, the work presented in the thesis is our own original work and we have positively cited the related work of the other researchers by clearly differentiating my work from their relevant work.

We further understand that if I am found guilty of any form of plagiarism in my thesis work even after my graduation, the institute reserves the right to revoke my BS degree. Moreover, the Institute will also have the right to publish my name on its website that keeps a record of the students who plagiarized in their thesis work.

This Institute reserves the right to publish our name on its website that keeps a record of the students who plagiarized in their thesis work.

---

Zuha Fatima

210201017

---

Humna Ali

210201013

I hereby acknowledge that submitted thesis is final version and should be scrutinized for plagiarism as per IST policy

---

Tufail Shah

Dated: \_\_\_\_\_

---

Verified by Plagiarism Cell Officer

Dated\_\_\_\_\_

Copyright © 2025

This document is jointly copyrighted by the authors and the Institute of Space Technology (IST). Both authors and IST can use, publish or reproduce this document in any form. Under the copyright law no part of this document can be reproduced by anyone, except copyright holders, without the permission of authors.

## ABSTRACT

Acne vulgaris is a common dermatological condition affecting up to 85% of individuals aged 12 to 24, often resulting in significant psychosocial impact. Accurate classification of lesion types such as nodules, papules, and pustules is critical for effective treatment, yet remains challenging due to overlapping visual features and limited access to dermatological expertise, especially in resource-limited settings.

This study introduces AcuCare, a lightweight and interpretable system for acne lesion classification and treatment suggestion. The proposed pipeline employs YOLOv8 for acne localization, followed by unsupervised segmentation using Fuzzy C-Means and K-Means clustering on CLAHE-enhanced Lab\* images. A diverse set of handcrafted features, including GLCM, LBP, Gabor filters, color histograms, and shape descriptors is extracted and used for classification via Extreme Learning Machine (ELM) and an ensemble variant. Performance is benchmarked against Support Vector Machine (SVM), Random Forest, K-Nearest Neighbors, and LightGBM.

Evaluation on a curated dataset of 184 labeled acne images demonstrates that SVM with FCM-based features achieves the highest test accuracy (88.0%), while Ensemble ELM offers robust, consistent performance across segmentation strategies. A prototype mobile application developed in Flutter enables on-device classification and treatment guidance.

The results highlight AcuCare’s potential as a scalable, accessible dermatological support tool suitable for low-resource environments.



# TABLE OF CONTENTS

1	INTRODUCTION .....	1
1.1	Project Vision .....	1
1.2	Problem Domain Overview .....	2
1.3	Problem Statement .....	3
1.4	Problem Elaboration.....	4
1.5	Goals and Objectives.....	6
1.6	Project Scope .....	7
2	Literature Review .....	9
2.1	Preprocessing in Dermatological Imaging .....	9
2.2	Acne Detection and Classification Approaches.....	9
2.3	Segmentation Techniques in Acne Imaging .....	10
2.4	Feature Extraction for Skin Lesion Analysis.....	11
2.5	Machine Learning Models for Dermatological Classification .....	11
2.6	Research Gaps and Open Challenges.....	11
2.7	Positioning of the Current Research .....	12
2.8	Summary of Reviewed Literature .....	12
3	Proposed Approach and Methodology.....	18

3.1	Dataset Preparation .....	19
3.1.1	Class Distribution .....	20
3.1.2	Data Splitting .....	20
3.2	Preprocessing and Color Space Enhancement .....	21
3.2.1	RGB to L*a*b Color Space Conversion .....	21
3.2.2	Contrast Enhancement using CLAHE .....	22
3.2.3	Preprocessing Effects on Segmentation .....	24
3.2.4	Output Format .....	24
3.3	Image Segmentation .....	25
3.3.1	K-means Clustering .....	25
3.3.2	Fuzzy C-Means (FCM) .....	26
3.3.3	Comparison and Justification .....	27
3.4	Feature Extraction .....	29
3.4.1	Texture features .....	30
3.4.2	Color Features .....	31
3.4.3	Shape Descriptors and Edge density .....	32
3.4.4	Frequency-Domain Features (Gabor Filters) .....	32
3.4.5	Final Feature Vectors .....	32
3.4.6	Feature Selection and Dimensionality Control .....	33
3.5	Classification .....	35

3.5.1	Classifiers Used.....	36
3.5.2	ELM Architecture and Training.....	37
3.5.3	Evaluation Setup .....	39
3.5.4	Comparative Classifiers.....	40
3.6	Results and Discussion.....	41
3.6.1	Performance on FCM-Segmented Data.....	41
3.6.2	Performance on K-Means Segmented Data.....	43
3.6.3	Comparative Discussion .....	44
4	Conclusion and Future work .....	48
4.1	Summary of Contributions .....	48
4.2	Key Findings.....	49
4.3	Limitation .....	49
4.4	Future Work.....	50
5	Project Deliverables .....	51
6	Ethical Considerations .....	52
6.1	Non-Diagnostic Intent .....	53
6.2	Bias and Generalizability .....	53
6.3	Privacy and Data Handling.....	53
6.4	Informed Usage.....	53

6.5 Responsibility and Future Development .....	54
References .....	55
Appendix .....	58
Appendix A: Flowchart.....	58
Appendix B: Use case Diagram .....	59

## LIST OF FIGURES

Figure 3.1: Flowchart of Methodology .....	19
Figure 3.2: Visualization of Preprocessing Pipeline and LAB Color Space Decomposition .....	23
Figure 3.3: Top 10 features selected from the K-means segmentation pipeline. ....	34
Figure 3.4: Top 10 most discriminative features (based on F-score) from the FCM pipeline. ....	35
Figure 3.5: Comparison of confusion matrices for ELM classifier using FCM (left) and K-Means (right) segmentation. ....	47
Figure 3.6: ROC curves for ELM classifier using FCM (left) and K-means (right)..	47

## LIST OF TABLES

Table 2.1: Literature Review and Summary Table.....	12
Table 3.1: Data Partition Summary .....	20
Table 3.2: Visual Comparison of Lesion Segmentation Using K-Means and Fuzzy C-Means (FCM).....	29
Table 3.3: Classification performance of models on FCM-segmented dataset.....	42
Table 3.4: Classification performance of models on K-means segmented dataset ....	44
Table 3.5: Confusion metrics for ELM (FCM vs KMeans) .....	46
Table 5.1: Project Deliverables .....	51

## **LIST OF ABBREVIATION & SYMBOLS**

ELM	Extreme Learning Machine
GLCM	Gray-Level Co-occurrence Matrix
FCM	Fuzzy C-Means
CLAHE	Contrast Limited Adaptive Histogram Equalization
LAB	Lightness, red/green axis, yellow/blue axis
RGB	Red, Green Blue
UI	User Interface
API	Application Programming Interface

# 1 INTRODUCTION

## 1.1 Project Vision

Acne vulgaris is one of the most common dermatological conditions worldwide, particularly prevalent among adolescents and young adults. Although not life-threatening, its visible nature and chronic course can lead to significant psychological distress, including anxiety, low self-esteem, and social withdrawal. Accurate identification of acne lesion types such as papules, pustules, and nodules is critical for effective treatment planning. However, clinical diagnosis is often limited by subjectivity, variability in lesion presentation, and the inaccessibility of dermatological expertise in underserved regions.

Recent advancements in artificial intelligence (AI) have enabled automated acne detection, yet many existing approaches rely heavily on deep learning models that demand large, annotated datasets and high computational power. These models often lack interpretability, making them unsuitable for resource-constrained deployment such as mobile health (mHealth) applications. Furthermore, they frequently overlook practical deployment challenges, including image segmentation quality, feature transparency, and device performance limitations.

This project proposes AcuCare, a real-time acne classification and treatment support system designed to function effectively under constrained resources. The solution integrates unsupervised image segmentation, interpretable handcrafted feature extraction, and ensemble learning techniques. AcuCare is deployed within a cross-platform mobile application developed using Flutter, delivering on-device acne assessment and over-the-counter (OTC) treatment guidance in a user-accessible format.



## 1.2 Problem Domain Overview

This study operates at the intersection of medical image analysis, machine learning, and mobile health (mHealth), with a specific focus on the automated classification of acne vulgaris lesions. Acne is a multifactorial skin disorder that is commonly presented as a combination of papules, pustules, nodules, and other lesion types. Clinical management relies heavily on accurate lesion categorization, as different types require distinct treatment approaches. Traditionally, this classification is performed by dermatologists through visual inspection, an approach that is inherently subjective, time-consuming, and often inaccessible due to geographic or financial barriers.

In recent years, machine learning has emerged as a powerful tool for supporting dermatological diagnostics. However, the majority of existing research emphasizes deep convolutional neural networks (CNNs), which, while effective in terms of accuracy, come with significant limitations. These include dependency on large-scale annotated datasets, lack of model interpretability, and high computational demands that restrict deployment to high-end servers or cloud-based platforms. Such characteristics make them impractical for real-time, on-device usage particularly in low-resource settings where connectivity and hardware capacity are limited.

Simultaneously, mHealth applications have gained prominence as scalable tools for self-assessment, treatment tracking, and early-stage diagnosis. Yet, most existing acne-related mobile applications are either overly simplistic (focusing solely on skincare advice) or adopt black-box models without providing interpretable feedback or personalized treatment guidance. Moreover, few, if any incorporate unsupervised segmentation, handcrafted feature engineering, and ensemble learning in an integrated mobile pipeline.

This gap presents an opportunity to develop an interpretable, lightweight, and accurate acne classification system tailored for real-world mHealth use. By leveraging unsupervised image segmentation, domain-specific feature extraction, and efficient classification models, this project addresses the limitations of current AI-driven dermatology solutions while enhancing accessibility and usability for end users.

### **1.3 Problem Statement**

Despite the high global prevalence of acne vulgaris affecting approximately 85% of individuals aged 12 to 24, accurate and accessible diagnosis remains a significant challenge. The clinical classification of acne lesions into categories such as nodules, papules, and pustules is essential for effective treatment planning. However, this process is often hindered by overlapping visual characteristics, intra-class variability, and the subjectivity inherent in manual dermatological assessments. These limitations are particularly pronounced in resource-limited settings where specialist care is not readily available.

While artificial intelligence (AI)-based diagnostic systems have demonstrated promising results, most rely on deep learning architectures that are computationally intensive, require extensive annotated datasets, and offer limited interpretability. These constraints render them unsuitable for real-time, on-device deployment in mobile health applications. Furthermore, many existing solutions stop at lesion classification and fail to offer actionable, user-specific treatment guidance.

There is a clear need for a system that can:

1. Accurately classify acne lesions into clinically relevant categories using limited data,
2. Operate under computational constraints typical of mobile devices,
3. Provide interpretable outputs, and

4. Extend beyond diagnosis to include evidence-based, over-the-counter (OTC) treatment recommendations.

This research aims to address these needs by developing a lightweight, interpretable acne analysis pipeline that integrates unsupervised segmentation, handcrafted feature extraction, and efficient classification models, with seamless deployment within a mobile application for real-time usage.

## **1.4 Problem Elaboration**

The accurate classification of acne lesions is a multi-stage problem that poses several technical and practical challenges. The first critical step, lesion segmentation, involves isolating acne regions from healthy skin, which is complicated by factors such as uneven lighting, diverse skin tones, and the subtle visual boundaries between lesions and surrounding tissue. While deep learning-based segmentation models (e.g., U-Net) exist, they are often data-hungry, computationally intensive, and impractical for deployment on mobile devices without cloud support.

To address these constraints, this project adopts unsupervised clustering techniques specifically, Fuzzy C-Means (FCM) and K-Means—applied to the LAB color space with CLAHE enhancement. However, unsupervised segmentation introduces its own challenges, such as sensitivity to noise, poor performance on images with multiple overlapping lesions, and lack of semantic awareness. These factors directly influence downstream processes, particularly feature extraction and classification accuracy.

Following segmentation, the system must extract features that effectively differentiate between lesion types, which often share similar shape, size, and color characteristics. This necessitates the use of a diverse set of handcrafted features, including:

1. Texture-based descriptors such as Gray-Level Co-occurrence Matrix (GLCM) and Local Binary Patterns (LBP),
2. Color features across RGB, HSV, and YCbCr spaces,
3. Shape and edge density metrics, and
4. Frequency-domain features such as Gabor filters.

Selecting and combining these features in a way that enhances class separability without overfitting is a non-trivial task, especially given the limited dataset size and potential class imbalance (e.g., fewer nodules compared to pustules or papules).

The classification stage also presents a trade-off between accuracy and efficiency. While deep learning classifiers may offer high accuracy, they are unsuitable for real-time mobile deployment. Lightweight alternatives like Extreme Learning Machine (ELM), Random Forests, and Support Vector Machines (SVM) offer faster inference and lower memory usage but must be carefully tuned to avoid underperformance.

Beyond classification, there exists a practical expectation from users for actionable output. Most existing tools stop at lesion identification, providing little guidance on next steps. Yet users often seek directions on treatment—what to apply, how often, and whether to consult a physician. This project addresses this unmet need by linking classification outputs to evidence-based over-the-counter (OTC) treatment recommendations specific to each acne type.

Finally, integrating the entire pipeline into a mobile application introduces additional engineering constraints: limited memory, real-time performance requirements, device variability, and user interface usability. The system must maintain high diagnostic fidelity while ensuring fast processing and seamless user experience without reliance on external servers or internet access.

## 1.5 Goals and Objectives

The primary goal of this research is to design and implement a lightweight, interpretable, and mobile-compatible system for the automated classification of facial acne lesions and the delivery of treatment recommendations. To achieve this, the project is structured around the following objectives:

1. **To implement an acne presence detection module** using a YOLOv8-based object detection API, ensuring that only relevant images proceed to the classification pipeline.
2. **To segment acne lesions using unsupervised clustering techniques**, specifically Fuzzy C-Means (FCM) and K-Means, applied to the LAB color space with CLAHE preprocessing for enhanced contrast and lesion boundary separation.
3. **To extract a comprehensive set of handcrafted features** from segmented regions, including texture descriptors (GLCM, LBP), color metrics (RGB, HSV, YCbCr), shape and edge density features, and frequency-domain filters (Gabor), to capture the visual characteristics of different lesion types.
4. **To classify lesions into three clinically meaningful categories: nodules, papules, and pustules** using a range of machine learning models, including Extreme Learning Machine (ELM), ensemble ELM, Random Forest, SVM, KNN, and LightGBM.
5. **To evaluate and compare classification performance** across both segmentation pipelines (FCM and K-Means) using metrics such as accuracy, per-class recall, confusion matrices, and ROC curves, thereby identifying the optimal configuration.
6. **To identify the dominant acne type in each processed image**, based on lesion frequency or proportional presence, as a basis for treatment logic.

7. **To link classification results with over-the-counter treatment recommendations**, providing users with actionable guidance tailored to their specific acne profile.
8. **To deploy the complete system within a cross-platform mobile application**, built using Flutter, integrating image input, server-side classification, result display, and treatment suggestions in a real-time, user-friendly interface.

These objectives collectively support the development of a scalable and accessible dermatological support tool that bridges the gap between self-assessment and clinical care, particularly in resource-constrained settings.

## 1.6 Project Scope

This project focuses on the development of a real-time, mobile-compatible system for the detection, classification, and treatment recommendation of acne vulgaris, specifically targeting three clinically relevant lesion types: nodules, papules, and pustules. The system, named AcuCare, is designed to function efficiently in resource-constrained environments, without reliance on cloud computing or high-end hardware.

The scope of the work includes:

- **Acne presence detection** using a pre-trained YOLOv8-based object detection API to screen incoming images.
- **Image segmentation** of acne lesions via two unsupervised clustering algorithms; Fuzzy C-Means (FCM) and K-Means applied to CLAHE-enhanced LAB color space to isolate lesion regions from background skin.
- **Handcrafted feature extraction** from segmented regions, incorporating texture (GLCM, LBP), color (RGB, HSV, YCbCr), shape, edge density, and frequency-domain (Gabor filter) features.

- **Classification** of lesions using multiple machine learning algorithms, with a primary focus on Extreme Learning Machine (ELM) and its ensemble variant, alongside Random Forest, SVM, KNN, and LightGBM for comparative evaluation.
- **Determination of dominant acne type** per image to guide personalized treatment output.
- **Recommendation of over-the-counter (OTC) treatments**, mapped to lesion type and designed for informational support.
- **Deployment of the complete pipeline within a Flutter-based mobile application**, integrating image input, back-end communication via Flask, real-time result visualization, and treatment guidance.

The system is trained and tested on a manually curated dataset of cropped facial acne images (150x150 pixels), containing 51 nodules, 61 papules, and 72 pustules, using a fixed 70/30 train-test split. No data augmentation is applied in this version.

## **2 LITERATURE REVIEW**

### **2.1 Preprocessing in Dermatological Imaging**

Medical image analysis has played a pivotal role in computer-aided dermatological diagnosis. The use of contrast enhancement to improve skin lesion segmentation has been shown to enhance boundary detection, although it may lack generalizability across diverse lesion types [1]. A hybrid model incorporating hair artifact removal was proposed for melanoma detection; however, its applicability to acne or other non-cancerous conditions remains unaddressed [2]. The relevance of color normalization in segmentation has also been demonstrated, although performance tends to degrade in complex skin backgrounds [3]. These studies underscore the foundational importance of preprocessing while highlighting the need for adaptable segmentation methods suited to a broader range of dermatological conditions.

### **2.2 Acne Detection and Classification Approaches**

Recent research has increasingly focused on AI-based approaches for acne classification. One study proposed a six-class acne disease recognition system that combines contrast enhancement, RGB-to-LAB color conversion, K-means clustering for segmentation, and a hybrid of GLCM and statistical feature extraction. The system achieved a classification accuracy of 98.50% using a Random Forest classifier on a dataset of 2,100 images [4]. While methodologically robust, the implementation relies on MATLAB and is not optimized for real-time, mobile deployment. Moreover, the system focuses solely on acne classification and does not incorporate treatment recommendations or support on-device inference.

A hybrid segmentation-classification pipeline for acne severity prediction was proposed using a combination of the Mayfly Optimization Algorithm (MOA) and Fuzzy C-Means (FCM) clustering, followed by GLCM-based texture feature extraction and classification via an Artificial Neural Network (ANN). The model emphasizes optimized



lesion segmentation using MOA-enhanced cluster centers, which significantly improved performance metrics over traditional classifiers. The system achieved an accuracy of 97%, outperforming SVM, KNN, and Naïve Bayes models in both precision and F1-score [5]. While the approach is innovative in its hybrid optimization technique, it targets severity grading (mild, moderate, severe) rather than lesion-type classification, and is not optimized for mobile or real-time use.

Ensemble neural networks have been employed to achieve high accuracy in acne detection; however, their reliance on large, annotated datasets limits scalability and generalization [4]. A joint acne grading and counting framework based on label distribution learning has also been introduced, providing detailed severity assessments but at the cost of substantial computational overhead [5]. A comparative analysis of segmentation techniques was conducted, though it did not result in a unified pipeline suitable for deployment [6]. Additionally, a CNN-based system called AcneNet demonstrated strong performance in acne class identification, but struggled to differentiate between mild and severe lesions [7].

Collectively, these studies highlight ongoing advances in automated acne classification, but also reveal key limitations particularly in terms of lightweight deployment, model interpretability, and the integration of post-diagnostic support such as treatment recommendations. These limitations motivate the current research toward a more mobile-compatible, interpretable, and actionable acne analysis system.

### **2.3 Segmentation Techniques in Acne Imaging**

Segmentation remains a key challenge in dermatological imaging due to low inter-class variance and overlapping boundaries. K-Means clustering has been combined with a firefly optimization algorithm to improve lesion extraction under uneven lighting; however, this approach underperformed on low-contrast images [8]. A modified CLAHE method was

applied to enhance contrast in kidney segmentation, suggesting the broader utility of CLAHE across medical domains, although its application to skin imaging remains underexplored [9]. These findings motivate the use of CLAHE-enhanced  $Lab^*$  color space in this project for unsupervised acne lesion segmentation.

## **2.4 Feature Extraction for Skin Lesion Analysis**

Effective classification requires robust feature extraction. Texture-based methods such as GLCM and LBP have been applied for melanoma classification with reliable results, although models tended to struggle when distinguishing visually similar classes [10]. GLCM and ELM were also used for acne type classification, achieving promising accuracy but with limited effectiveness on images exhibiting low texture contrast [15]. A severity grading model tailored specifically to the Chinese population has further raised concerns regarding demographic generalizability [11]. These studies validate the relevance of handcrafted features while also highlighting their sensitivity to image quality and dataset bias.

## **2.5 Machine Learning Models for Dermatological Classification**

Machine learning has been widely adopted in dermatology due to its balance between performance and interpretability. Convolutional Extreme Learning Machines (CELM) have been evaluated and found efficient for image classification, although they exhibit limitations when applied to complex datasets [12]. SURF features combined with K-Nearest Neighbors (KNN) have also been used for acne detection, offering computational simplicity but lacking scalability [13]. A chronic acne treatment tracker based on image analysis has been developed, though it required manual input, thereby reducing the level of automation [14]. These works support the potential of ELM and other lightweight classifiers in skin imaging tasks, particularly when integrated with mobile platforms.

## **2.6 Research Gaps and Open Challenges**

Despite promising results in prior studies, several limitations persist. Many models rely on large-scale or population-specific datasets, reducing generalizability. There is limited emphasis on distinguishing between acne types (as opposed to severity grades), and few systems integrate lesion classification with actionable treatment guidance. Moreover, most existing solutions are either server-based or require manual preprocessing steps, making them unsuitable for seamless mobile deployment.

## 2.7 Positioning of the Current Research

This research addresses the aforementioned gaps by proposing a real-time, interpretable acne analysis system built for mobile devices. Key contributions include:

1. **Segmentation:** Application of Fuzzy C-Means and K-Means clustering on CLAHE-enhanced LAB space to isolate acne lesions without supervised training.
2. **Feature Engineering:** Use of handcrafted features (GLCM, LBP, Gabor filters, RGB/HSV/YCbCr color descriptors, and shape metrics) to capture lesion characteristics.
3. **Classification:** Evaluation of ELM and other lightweight classifiers (RF, SVM, LightGBM) with cross-validation to ensure efficiency and interpretability.
4. **Deployment:** End-to-end integration within a Flutter mobile app that delivers both diagnosis and tailored over-the-counter treatment recommendations.

By combining unsupervised segmentation, handcrafted feature analysis, and efficient classifiers into a mobile-first pipeline, this research aims to bridge the gap between academic models and real-world acne self-assessment tools

## 2.8 Summary of Reviewed Literature

Table 2.1: Literature Review and Summary Table

The table provides a concise overview of the key findings from the literature review.

No	Name, Reference	Authors	Year	Input	Output	Description
1	Colour and contrast enhancement for improved skin lesion segmentation [1]	Schaefer et al.	2011	Skin lesion images	Enhanced segmentation	Improves color and contrast for better segmentation of skin lesions.
2	Detection of melanoma with hybrid learning method [2]	Suiçmez et al.	2023	Dermoscopic images	Accurate melanoma detection	Combines wavelet transform and hair artifact removal techniques.
3	Effect of color feature normalization on segmentation [3]	Khan et al.	2016	Color images	Improved segmentation	Uses color feature normalization for better boundary clarity.
4	In-depth analysis of automated	Ahsan et al.	2025	Acne images	Multi-class acne classification	Uses RGB-LAB, K-Means, GLCM + stats,

	acne recognition and classification [4]					and Random Forest (98.50%).
5	Acne detection by ensemble neural networks [5]	Zhang and Ma	2022	Acne images	Accurate acne detection	Ensemble neural networks used for acne lesion recognition.
6	Joint acne image grading and counting via label distribution learning [6]	Wu et al.	2019	Acne images	Severity grading and lesion count	Uses label distribution learning for detailed acne assessment.
7	Segmentation of acne vulgaris image techniques [7]	Moncho- Santonja et al.	2023	Acne images	Comparative study	Benchmarks segmentation methods without a unified pipeline.
8	AcneNet – CNN-based acne class	Junayed et al.	2019	Acne images	Class identification	CNN-based acne classifier with

	classification [7]					challenges in severity distinction.
9	K-Means + firefly optimization for skin lesion segmentation [8]	Garg and Jindal	2021	Skin lesion images	Improved lesion segmentation	Combines K-Means and firefly algorithm for enhanced precision.
10	CNN-based kidney segmentation using modified CLAHE [9]	Buriboev et al.	2024	Medical images	Improved segmentation	Uses CLAHE to enhance contrast; promising for dermatology.
11	Skin tumor detection using texture analysis [10]	Almeida and Santos	2020	Tumor images	Reliable classification	Uses GLCM and LBP for melanoma and nevus differentiation.
12	Acne vulgaris type classification using GLCM + ELM [15]	Hasanah et al.	2022	Acne images	Acne type classification	Uses texture features and ELM; poor performance

						on low-contrast skin.
13	Severity grading model tailored to Chinese population [11]	Gao et al.	2025	Acne images	Acne severity grading	Model lacks demographic generalization outside Chinese data.
14	Review of CELM for dermatological image classification [12]	Rodrigues et al.	2021	Dermatological images	Efficient classification	Evaluates CELM as lightweight alternative to traditional CNNs.
15	Acne detection using SURF + KNN [13]	Kittigul and Uyyanonvara	2017	Acne images	Effective but non-scalable detection	Uses SURF for feature extraction and KNN for classification.
16	Tracking chronic acne treatment via image analysis [14]	Lucut and Smith	2016	Acne treatment images	Response tracking	Requires manual annotation, limiting full automation.

17	Acne lesion, scar, and normal skin classification [16]	Ramli et al.	2011	Acne images	Multi-state classification	Differentiates between acne, scarring, and normal skin regions.
18	Mobile-based acne lesion classification [17]	Alamdari et al.	2016	Acne images	Android-compatible acne detection	Developed mobile app for acne classification with basic accuracy.



### 3 PROPOSED APPROACH AND METHODOLOGY

This chapter outlines the complete methodology adopted for automated acne classification based on segmented facial lesion regions. The proposed pipeline is designed to operate under lightweight computational constraints while maintaining accuracy and interpretability. It consists of four main phases: **preprocessing**, **segmentation**, **feature extraction**, and **classification**. The system is trained to distinguish between three clinically significant acne types: **nodules**, **papules**, and **pustules**.

The methodology leverages unsupervised segmentation techniques (K-means and Fuzzy C-Means), handcrafted feature descriptors (including GLCM, LBP, color, and shape metrics), and multiple machine learning classifiers (ELM, RF, SVM, KNN). Figure 1 illustrates the sequential workflow of the system, from dataset preparation to final acne type prediction.

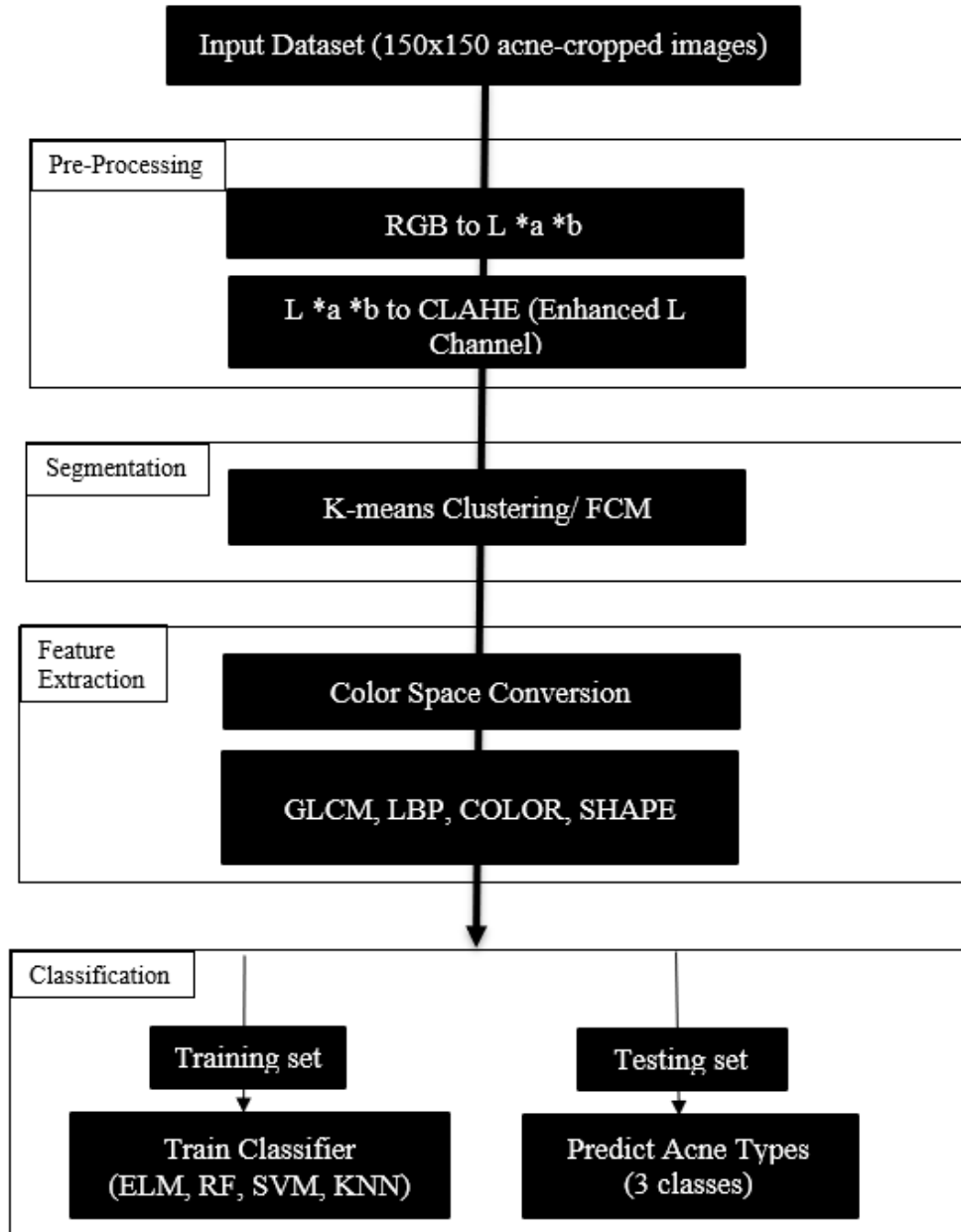


Figure 3.1: Flowchart of Methodology

The flowchart illustrates the sequence of processing steps.

### 3.1 Dataset Preparation

The dataset used in this study consists of manually curated and annotated images of facial acne lesions collected from multiple publicly available sources, including Skin90, DermNet, and selected online dermatology repositories. To ensure consistency across the

pipeline and reduce background noise, each image was manually cropped to 150×150 pixels, centering the region of interest containing visible acne lesions.

### 3.1.1 Class Distribution

The dataset was designed to support three clinically relevant acne categories: nodules, papules, and pustules. A total of 184 images were collected, with the following distribution:

- **Nodules:** 51 images
- **Papules:** 61 images
- **Pustules:** 72 images

No image augmentation was applied in the current version of the pipeline to preserve the natural variation in lesion morphology, lighting conditions, and skin tone. This setup allows the model to generalize under real-world conditions, albeit at the cost of a relatively limited sample size.

### 3.1.2 Data Splitting

The dataset was split into training (70%) and testing (30%) subsets using stratified sampling to maintain class proportions across both sets. This ensures balanced representation of all lesion types in both phases of the classification task. The splits are as follows:

Table 3.1: Data Partition Summary

This table presents the distribution of images across training and testing sets for each acne class.

<b>Class</b>	<b>Total</b>	<b>Training (70%)</b>	<b>Testing (30%)</b>
Nodules	51	36	15
Papules	61	43	18

Pustules	72	50	22
<b>Total</b>	<b>184</b>	<b>129</b>	<b>55</b>

Each image was normalized and formatted consistently prior to pipeline input, and file naming conventions were preserved to allow traceability during prediction visualization and confusion matrix analysis.

### 3.2 Preprocessing and Color Space Enhancement

The preprocessing stage in this study is designed to enhance image quality and ensure uniformity across the input dataset prior to segmentation. Given the variability in lighting conditions, skin tones, and lesion contrast present in facial acne images, preprocessing is essential to normalize luminance, suppress background noise, and improve the visual distinction of acne regions from surrounding skin. The preprocessing phase in this study involves two key operations:

1. Color space conversion from RGB to  $L^*a^*b$
2. Contrast enhancement using CLAHE (Contrast Limited Adaptive Histogram Equalization)

#### 3.2.1 RGB to $L^*a^*b$ Color Space Conversion

The RGB color space, while standard for digital images, is not perceptually uniform and does not separate luminance from chromatic components. This separation is essential when targeting contrast-specific enhancements or segmentation tasks that depend on intensity variations.

To overcome these limitations, all input images are converted to the  $L^*a^*b$  color space, where:

- $L^*$  represents Luminance

- $a^*$  corresponds to green-red color spectrum
- $b^*$  represents the blue-yellow color spectrum

This transformation allows the contrast enhancement to operate selectively on the luminance channel ( $L^*$ ), preserving color integrity while improving boundary definition.

The conversion is performed using the standard formula:

$$\begin{bmatrix} X \\ Y \\ Z \end{bmatrix} = \begin{bmatrix} 0.4124 & 0.3576 & 0.1805 \\ 0.2126 & 0.7152 & 0.0722 \\ 0.0193 & 0.1192 & 0.9505 \end{bmatrix} \begin{bmatrix} R \\ G \\ B \end{bmatrix}$$

The resulting XYZ values are then converted to  $L^*a^*b$  using standard nonlinear transformations defined by the CIE76 specification. The final  $L^*a^*b$  representation allows for separation of luminance and chromatic components, facilitating contrast enhancement and segmentation in subsequent stages.

### 3.2.2 Contrast Enhancement using CLAHE

Following color space conversion, local contrast is enhanced using Contrast Limited Adaptive Histogram Equalization (CLAHE). CLAHE operates by dividing the  $L^*$  channel into small contextual regions (tiles), performing histogram equalization within each, and limiting contrast amplification via a clip threshold. This technique is particularly effective in medical imaging, as it improves visibility in poorly illuminated regions while preserving edge information and suppressing noise over-amplification [10].

In this study, CLAHE was configured with a clip limit of 2.0 and a tile grid size of  $8 \times 8$  pixels. These parameters were empirically chosen to maximize boundary definition in acne lesions especially papules and pustules without overexposing homogeneous regions. After enhancement, the modified  $L^*$  channel was recombined with the original  $a^*$  and  $b^*$  components to produce a contrast-enhanced  $L^*a^*b$  image, which was then used for segmentation.

To address the variability in illumination and lesion contrast, the input images were first denoised using a bilateral filter to preserve edges while smoothing background textures. Following this, the color space was converted from RGB to Lab, separating luminance from chromaticity. The  $L^*$  channel was selectively enhanced using Contrast Limited Adaptive Histogram Equalization (CLAHE) to improve local contrast in lesion regions.

Figure 2 illustrates each preprocessing stage. The  $a^*$  and  $b^*$  channels further expose chromatic variance between lesion and surrounding skin, which is leveraged in segmentation (e.g.,  $b^*$  thresholding for pus detection). Enhancing the  $L^*$  channel independently preserves color integrity while making acne lesions more distinguishable from skin texture.

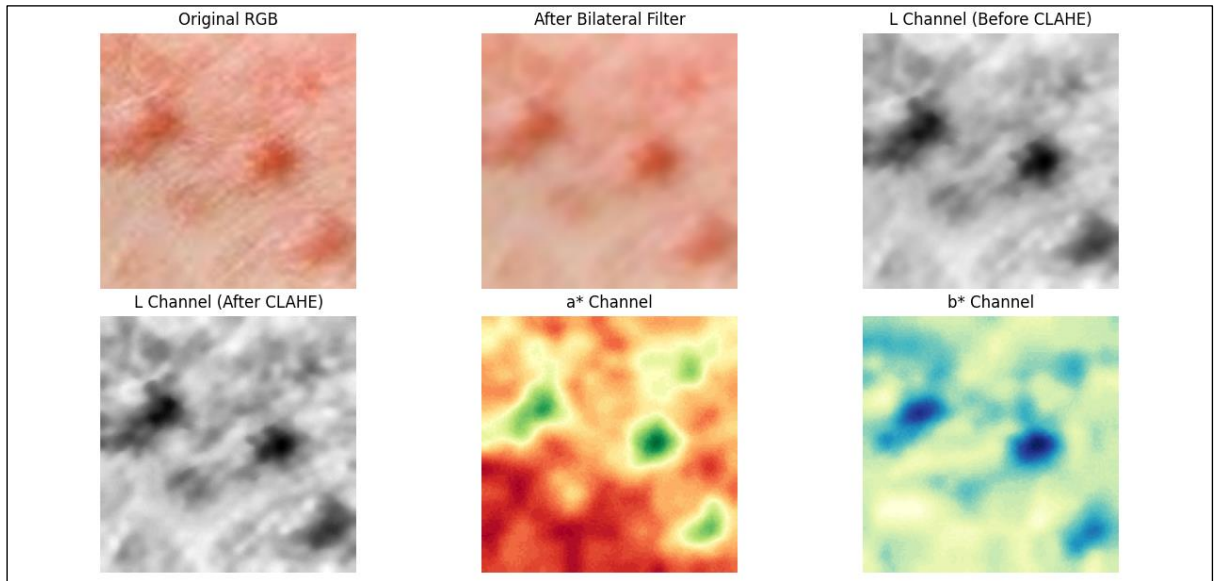


Figure 3.2: Visualization of Preprocessing Pipeline and LAB Color Space

#### Decomposition

*This figure illustrates the key preprocessing stages applied prior to segmentation. The top row shows the original RGB input, the result of bilateral filtering for edge-preserving denoising, and the luminance ( $L^*$ ) channel extracted from the  $L^*a^*b^*$  color space before contrast enhancement. The*

*bottom row displays the CLAHE-enhanced  $L^*$  channel, the  $a^*$  channel (representing the green–red chromatic axis), and the  $b^*$  channel (blue–yellow axis).*

*The enhanced  $L^*$  channel improves boundary clarity in lesion regions, while the  $a^*$  and  $b^*$  channels expose chromatic variations leveraged in acne-specific segmentation logic such as pus detection via  $b^*$  thresholding*

### **3.2.3 Preprocessing Effects on Segmentation**

Both K-means and Fuzzy C-Means (FCM) clustering techniques rely heavily on pixel-level feature similarity for accurate segmentation. The use of CLAHE-enhanced  $L^*a^*b$  images significantly improves segmentation quality by enhancing luminance contrast, which is especially beneficial for clustering algorithms. In the case of K-means, the enhanced  $L^*$  channel provides better separation of lesion intensities in the Euclidean feature space, resulting in more distinct and stable cluster centroids. For FCM, the suppression of local brightness variability leads to a reduction in membership ambiguity, producing cleaner and more coherent soft clustering results.

In the absence of preprocessing, segmentation often suffers from poor lesion-background separation. Low-contrast papules, in particular, tend to blend with surrounding skin, making accurate clustering difficult. Moreover, uneven illumination across the face can cause over-segmentation, where non-lesion regions are mistakenly identified as acne. This ultimately results in unreliable feature maps for downstream processes such as texture extraction and classification.

### **3.2.4 Output Format**

Following the preprocessing phase, all images are retained in the  $L^*a^*b$  color space,

with the  $L^*$  channel enhanced using CLAHE. Segmentation is subsequently performed either on the  $L^*$  channel alone or on the full  $L^*a^*b$  image, depending on the segmentation method applied. Grayscale conversion is deferred until the feature extraction stage, where texture-based descriptors such as GLCM and LBP require single-channel input. Throughout this process, file naming conventions and class labels are preserved to ensure traceability during training, testing, and evaluation. This standardized preprocessing pipeline ensures consistent input quality, which in turn improves the accuracy and robustness of both segmentation and classification stages.

### **3.3 Image Segmentation**

The segmentation stage plays a crucial role in isolating acne lesion regions from surrounding healthy skin. Accurate segmentation directly influences the quality of feature extraction and the effectiveness of subsequent classification. This study explores and compares two unsupervised clustering methods for segmentation: K-means clustering and Fuzzy C-Means (FCM). Both techniques are applied to the preprocessed images in the  $L^*a^*b$  color space, which enhances lesion boundary contrast and enables better separation based on pixel-level similarity.

#### **3.3.1 K-means Clustering**

K-means clustering is a widely adopted unsupervised learning algorithm that partitions an image into  $K$  clusters by minimizing intra-cluster variance based on Euclidean distance. In this study, K-means is applied to the  $L^*a^*b$  color space of the preprocessed image, where each pixel is treated as a three-dimensional feature vector composed of luminance and chromaticity components. The  $L^*a^*b$  space was selected for its perceptual uniformity, which allows for better separation of acne lesions from surrounding skin, as demonstrated in prior dermatological studies [3], [4].



The number of clusters  $\mathbf{K}$  is set to 3, based on the assumption that facial skin, background, and acne lesions can be segmented into three distinct regions. This cluster count aligns with approaches taken in earlier acne segmentation research, where authors achieved promising results using similar assumptions [4], [9]. Following clustering, the appropriate lesion-representing cluster is selected using a heuristic that prioritizes clusters with lower average luminance ( $L^*$ ) and elevated  $a^*/b^*$  values, which tend to correspond to inflamed or reddish acne regions. This strategy mirrors the post-clustering selection logic described by Garg and Jindal [9] in the context of skin region segmentation.

While K-means offers computational efficiency and is suitable for real-time mobile deployment, its reliance on hard clustering limits its ability to handle images with gradual lesion boundaries or noisy contrast. These limitations motivate the exploration of alternative soft clustering approaches such as Fuzzy C-Means.

Equation 1: K-Means Clustering Objective Function

$$J = \sum_{i=1}^k \sum_{x \in C_i} \|x - \mu_i\|$$

Where  $C_i$  is the cluster and  $\mu_i$  is the centroid

### 3.3.2 Fuzzy C-Means (FCM)

Fuzzy C-Means (FCM) is a soft clustering technique that extends the K-means algorithm by allowing each data point to belong to multiple clusters with varying degrees of membership. This feature is particularly advantageous for dermatological image segmentation, where acne lesion boundaries are often diffuse and pixel intensities transition gradually. Unlike hard clustering, FCM minimizes an objective function weighted by the fuzzy membership of

each pixel to the cluster centroids, thus preserving boundary uncertainty and spatial ambiguity.

In this study, FCM is applied to the same CLAHE-enhanced L\*a\*b image, with the number of clusters set to  $C=3$ , and a fuzzifier value  $m=2$ . The selection of the lesion-representing cluster is guided by analyzing the spatial distribution of membership values and their corresponding luminance characteristics, a technique inspired by soft lesion detection strategies in prior literature [6], [7].

Notably, Pandit and Chavan [5] utilized an FCM-based segmentation pipeline for acne severity analysis and demonstrated that soft clustering combined with optimized cluster selection significantly improves downstream classification accuracy. Their work supports the use of FCM in acne-focused applications, particularly where lesion morphology varies considerably in size and intensity. Compared to K-means, FCM demonstrated greater resilience to lighting inconsistencies and was particularly effective in identifying early-stage or shallow lesions such as papules.

Equation 2: FCM Objective Function

$$J_m = \sum_{i=1}^c \sum_{j=1}^n u_{ij}^m \|x_j - v_i\|^2$$

Where  $\|x_j - v_i\|^2$  is the Euclidean distance between  $x_j$  and  $v_i$ . Also,  $n$  is the number of data points in  $i$  clusters and  $c$  is the number of cluster centers.

### 3.3.3 Comparison and Justification

To evaluate the effectiveness of acne lesion segmentation, both K-Means and Fuzzy C-Means (FCM) clustering were applied across varied acne types and imaging conditions.

K-Means clustering offers the advantage of computational efficiency and is well-suited

for real-time applications. However, it assumes hard class boundaries, which can lead to fragmented or incomplete lesion masks in cases where lesion-to-skin contrast is low or boundaries are not sharply defined.

In contrast, FCM enables soft clustering, allowing a single pixel to belong to multiple clusters with varying degrees of membership. This characteristic makes it more robust to intensity overlap and better suited to lesions with soft or faded edges, which are common in acne, especially papules and pustules with blurred borders or pus diffusion.

As shown in the visual comparison:

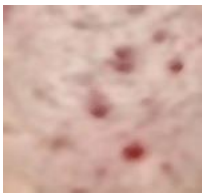


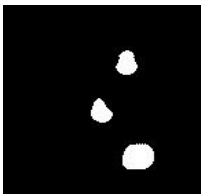
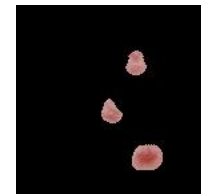








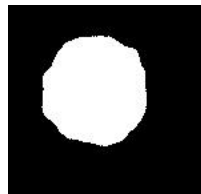

- For the papule image, K-Means produced a highly localized but limited mask, while FCM captured multiple lesion regions more effectively.
- In the second pustule case, K-Means yielded a broken and noisy contour, whereas FCM provided a smoother and more complete lesion mask.
- The third pustule example shows K-Means preserving the general lesion shape, but with internal gaps. FCM, after hole filling, preserved the full structure including the white center region, leading to a more medically realistic representation.

Empirical results suggest that FCM provides better lesion isolation in low-contrast or irregular illumination scenarios. While K-Means is retained in the pipeline for its speed and performance in well-lit images, FCM is more reliable for accurate boundary delineation.

Therefore, both methods are preserved for comparative evaluation, enabling the system to adapt based on image characteristics and supporting the potential development of ensemble-based segmentation strategies in future iterations.

Table 3.2: Visual Comparison of Lesion Segmentation Using K-Means and Fuzzy C-Means (FCM)

This table presents Comparison of preprocessed input, lesion masks, and segmentation results for different acne types using K-Means and FCM clustering methods.

Acne type	Preprocessed Image	Lesion Mask (K-means)	Segmentation Result (K-means)	Lesion Mask (FCM)	Segmentation Result (FCM)
Papule					
Pustule					
Nodule					

### 3.4 Feature Extraction

Following segmentation, the isolated lesion regions are subjected to feature extraction to generate discriminative representations suitable for classification. Given the limited size of

the dataset and the goal of maintaining model interpretability and computational efficiency, this study adopts a handcrafted feature approach. The selected features are designed to capture relevant textural, color, shape, and frequency-domain characteristics of acne lesions, enabling differentiation between nodules, papules, and pustules.

The feature extraction process operates on the masked lesion regions obtained from either K-means or Fuzzy C-Means segmentation. These masks are applied to the original RGB image, and the resulting cropped region of interest (ROI) is then converted to grayscale for texture analysis. The final feature set comprises descriptors from four main categories: texture features, color features, shape descriptors, and frequency-domain features.

### 3.4.1 Texture features

To capture the spatial and structural patterns of lesion surfaces, two complementary texture descriptors are used: Gray-Level Co-occurrence Matrix (GLCM) and Local Binary Pattern (LBP).

The GLCM is a second-order statistical method that quantifies pixel intensity relationships across specific spatial distances and angles. Four GLCM-based features are computed: Contrast, Correlation, Energy, and Homogeneity, extracted at a distance of 1 pixel across four angles ( $0^\circ$ ,  $45^\circ$ ,  $90^\circ$  and  $135^\circ$ ), resulting in a total of 16 features. These properties have been widely used in medical image analysis for capturing lesion surface roughness and regularity [6], [7].

Equation 3

$$\text{Contrast} = \sum_{i,j} (i - j)^2 P(i, j)$$

Equation 4

$$\text{Energy} = \sum_{i,j} P(i,j)^2$$

Equation 5

$$\text{Correlation} = \sum_{i,j} \frac{(i - \mu_i)(j - \mu_j) \cdot P(i,j)}{\sigma_i \cdot \sigma_j}$$

LBP encodes local texture by thresholding the neighborhood of each pixel against its center, producing binary patterns. The LBP histogram reflects the distribution of texture primitives and is particularly robust to illumination changes. In this study, uniform LBP with radius  $R=1$  and  $P=8$  sampling points is used to generate a compact yet expressive descriptor [6].

Equation 6

$$LBP_{P,R} = \sum_{p=0}^{P-1} s(g_p - g_c) \cdot 2^p$$

### 3.4.2 Color Features

Color descriptors are extracted from multiple color spaces to capture lesion pigmentation and inflammation levels. Mean and standard deviation values are computed for each channel in the RGB, HSV, and YCbCr color spaces, resulting in a total of 18 color features. The inclusion of these spaces provides complementary information: RGB preserves raw color, HSV isolates hue and saturation, and YCbCr separates luminance from chrominance components.

This multi-space color profiling enables the model to detect subtle chromatic differences across acne types, such as the reddish hue of papules or the yellowish core of pustules.

### 3.4.3 Shape Descriptors and Edge density

To quantify lesion morphology, shape-based features are extracted using binary masks of the segmented regions. These include:

1. Area: Number of pixels in the lesion region,
2. Perimeter: Total boundary length,
3. Circularity: Defined as  $4\pi \times \frac{Area}{Perimeter^2}$ , which reflects how round the lesion is,
4. Extent: Ratio of lesion area to the bounding box area.

In addition, edge density is computed using the Canny edge detector, which calculates the ratio of edge pixels to total pixels in the lesion mask. This feature captures sharpness and boundary detail that may correlate with lesion type severity.

### 3.4.4 Frequency-Domain Features (Gabor Filters)

To extract multi-scale and multi-orientation texture information, Gabor filters are applied to the grayscale ROI. Gabor filters are particularly effective in detecting oriented structures and repeated patterns, making them suitable for differentiating nodules from pustules. A total of 16 filters are used, covering four orientations ( $0^\circ, 45^\circ, 90^\circ$  and  $135^\circ$ ) across four spatial frequencies. The mean and standard deviation of each filtered response are computed, yielding a set of 32 frequency-domain features [6].

### 3.4.5 Final Feature Vectors

The final feature vector consists of 49 features extracted from each segmented lesion region. This includes:

1. 16 GLCM features,

2. 10 LBP + grayscale intensity statistics (mean, variance, skewness, kurtosis),
3. 18 color features,
4. 4 shape features + 1 edge density,
5. 16 Gabor features.

This combination ensures that both appearance and structure are comprehensively represented, while maintaining dimensionality low enough to avoid overfitting on limited data. All features are normalized using **z-score standardization**, and a **feature selection step** (SelectKBest) is applied during model training to retain the most informative attributes

### 3.4.6 Feature Selection and Dimensionality Control

To mitigate the risk of overfitting and reduce computational complexity, a feature selection step was incorporated following the extraction of handcrafted features. The SelectKBest method, using ANOVA F-score as the statistical criterion, was employed to assess the discriminative power of each feature in relation to the target class labels. This filter-based approach ranks features independently and selects the top-k candidates based on their individual F-scores, ensuring that only the most relevant and informative features are retained for classification.

Given the inherent differences in segmentation characteristics between the two pipelines, feature selection strategies were adapted accordingly. In the K-means segmentation pipeline, where lesion boundaries tend to be less precise and more prone to noise, a dimensionality reduction step was applied. Specifically, the top 10 features out of the original 49 were retained through cross-validation, striking a balance between model performance and generalization. These selected features predominantly included Gabor responses, edge density, GLCM metrics, and shape descriptors, reflecting a diverse representation of texture, structure, and frequency-domain information, as illustrated in Figure 3.



In contrast, the FCM segmentation pipeline demonstrated more consistent and accurate lesion boundary delineation, which preserved richer morphological and chromatic details. As a result, the full 49-feature set was retained during classification, as empirical tests showed that dimensionality reduction in this context led to a decline in predictive performance.

All features were standardized using z-score normalization prior to classification to ensure uniform scaling across descriptors. Importantly, feature selection was applied independently for each pipeline to preserve segmentation-specific feature dynamics and enable a fair comparative evaluation.

Visualizations of the selected features (Figures 3 and 4) further confirm the central role of LBP variance, edge density, and GLCM-based descriptors in both segmentation approaches. Structural attributes such as circularity, solidity, and extent, alongside specific Gabor filter responses, also ranked highly in the K-means pipeline, highlighting their discriminative value in acne lesion classification.

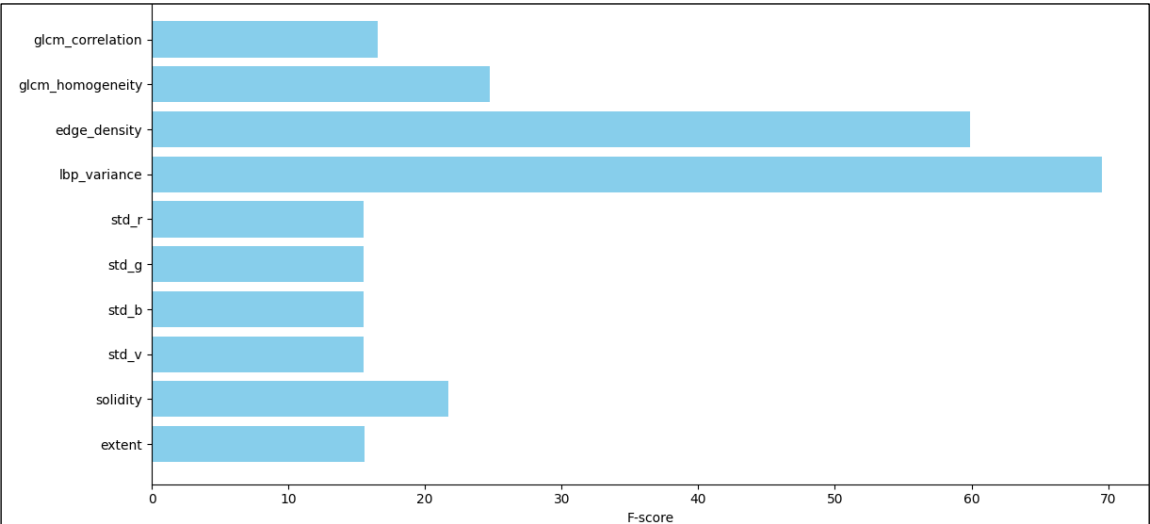


Figure 3.1: Top 10 features selected from the K-means segmentation pipeline.

Features are selected using SelectKBest and ranked by ANOVA F-score

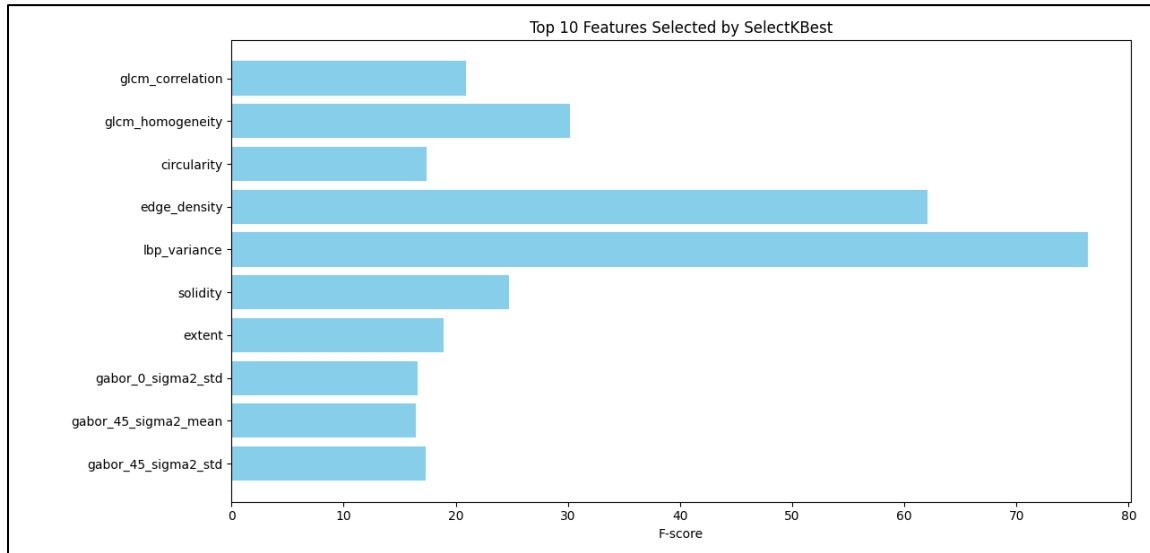


Figure 3.2: Top 10 most discriminative features (based on F-score) from the FCM pipeline.

All 49 features were used for classification; only the top 10 are shown for interpretability

### 3.5 Classification

The primary objective of the classification module is to automatically categorize acne lesions into one of three clinically significant types: nodules, papules, and pustules. This classification is performed using handcrafted feature vectors extracted from preprocessed and segmented images. The task is framed as a supervised multi-class classification problem, where each input feature vector corresponds to a labeled acne lesion type.

After segmentation and feature extraction (detailed in Sections 3.3 and 3.4), the feature vectors were normalized and reduced via feature selection techniques to retain only the most discriminative attributes. These optimized feature sets were then used to train various machine

learning classifiers.

Two distinct segmentation pipelines—Fuzzy C-Means (FCM) and K-Means clustering—were used to isolate the lesion regions, resulting in two independent feature datasets. Each dataset was evaluated across a range of classification models to assess the impact of segmentation quality on classification performance. All classifiers were trained and tested using the same data split (70% training, 30% testing) to ensure consistency and fair comparison.

This classification component is critical for enabling personalized treatment recommendations, as each acne type requires different therapeutic interventions. Accurate classification also enhances the interpretability and diagnostic reliability of the proposed system

### **3.5.1 Classifiers Used**

To identify the most effective approach for acne lesion classification, multiple supervised machine learning models were employed. Each model was trained on two sets of features: one derived from Fuzzy C-Means (FCM) segmented regions and the other from K-Means segmentation. This dual evaluation helped assess the robustness of each classifier across different preprocessing pipelines.

The classifiers used in this study include:

- **Extreme Learning Machine (ELM):** A single-layer feedforward neural network (SLFN) known for its extremely fast training speed. ELM randomly initializes input weights and analytically solves for output weights using a closed-form solution. It served as the primary model for this system.
- **Ensemble ELM:** To improve stability and reduce variance, an ensemble of 15 ELM models was implemented. Predictions were aggregated using a majority voting

mechanism, enhancing generalization and mitigating overfitting in small data scenarios.

- Support Vector Machine (SVM): A powerful classifier effective in high-dimensional spaces. The SVM model used a Radial Basis Function (RBF) kernel and was optimized via grid search over parameters  $C$  and  $\gamma$ .
- Random Forest (RF): An ensemble-based decision tree classifier that uses bagging and random feature selection to improve accuracy and control overfitting. It is robust to noise and particularly effective for structured tabular data.
- K-Nearest Neighbors (KNN): A simple, non-parametric method that classifies samples based on the majority label of their nearest neighbors. The value of  $K$  and distance metric were tuned through cross-validation.
- Light Gradient Boosting Machine (LightGBM): A gradient boosting framework based on decision trees that is optimized for speed and memory efficiency. LightGBM was configured with shallow depth and regularization to prevent overfitting.

Each model was evaluated using a 70/30 train-test split, and performance was compared across both segmentation pipelines. Hyperparameters for all models were selected using k-fold cross-validation to ensure optimal performance and generalizability

### **3.5.2 ELM Architecture and Training**

The Extreme Learning Machine (ELM) was adopted as the primary classification algorithm due to its computational efficiency, fast training time, and good generalization capability. ELM is a type of single-layer feedforward neural network (SLFN) where the input weights and biases are randomly initialized and remain fixed. Only the output weights are computed analytically using a closed-form solution, eliminating the need for iterative backpropagation.

## Modal Structure

Given an input feature vector  $x \in \mathbb{R}^n$ , the ELM transforms it using a hidden layer with randomly assigned parameters. The activation output of the hidden layer is then linearly combined using learned output weights  $\beta$  to produce the final prediction.

The ELM output function is defined as:

Equation 7

$$f(x) = \sum_{i=1}^L \beta_i \cdot h_i(x)$$

Where:

- $L$  is the number of hidden neurons
- $h_i(x)$  is the output of the  $i^{th}$  hidden neuron
- $\beta_i$  is the output weight corresponding to the neuron

In the matrix form:

Equation 8

$$H\beta = T \Rightarrow \beta = H^+T$$

Where:

- $H \in \mathbb{R}^{N \times L}$  is the hidden layer output matrix
- $T \in \mathbb{R}^{N \times m}$  is the target output matrix
- $H^+$  is the Moore–Penrose pseudoinverse of matrix  $H$

During training, the following steps were performed:

1. Random initialization of input weights and biases for hidden neurons

2. Computation of the hidden layer output matrix  $H$
3. Calculation of the output weight matrix  $\beta$  using pseudoinverse

Hyperparameters tuned during cross-validation include:

- Number of hidden neurons  $L$ : tested from 20 to 100
- Activation function: ReLU and sigmoid were compared
- Regularization constant CCC: values tested from 0.1 to 100

### 3.5.3 Evaluation Setup

To rigorously assess the performance of the proposed classification pipeline, a stratified evaluation strategy was adopted, ensuring balanced representation of all acne types (nodules, papules, pustules) across training and testing subsets. The dataset was split using a 70/30 ratio, with stratified sampling based on class labels to preserve proportional distribution.

No data augmentation techniques were applied to artificially inflate the dataset, as the objective was to assess model generalizability under real-world, unaltered conditions. While this introduced some limitations in sample diversity, it ensured that model performance metrics remained grounded in natural clinical variability, including differences in lighting, skin tone, and lesion morphology.

All classification models were evaluated using the same fixed splits for fair comparison across pipelines. To prevent information leakage, preprocessing, segmentation, feature extraction, and feature selection were applied exclusively within the training and testing boundaries. For models involving feature selection (e.g., SelectKBest for K-means), selection was performed solely on the training set, and the same features were subsequently applied to the test set.

Performance was quantified using the following evaluation metrics:

- Accuracy: The overall proportion of correct predictions across all classes.

- Precision, Recall, and F1-Score (per class): To assess model sensitivity and reliability across each acne type.
- Confusion Matrix: For analyzing class-wise prediction trends and misclassification patterns.
- Receiver Operating Characteristic (ROC) Curves and Precision-Recall (PR) Curves: Where applicable, these curves were used to visualize model confidence and discrimination across classes.

All models were trained and tested independently for both segmentation pipelines (K-means and FCM), and their results are presented comparatively in Section 3.6.

#### **3.5.4 Comparative Classifiers**

To validate the performance of the proposed ELM classifier, multiple widely-used machine learning models were implemented for comparative evaluation. These include Support Vector Machine (SVM), Random Forest (RF), k-Nearest Neighbors (KNN), and Light Gradient Boosting Machine (LightGBM). Each model was trained and evaluated using the same preprocessed feature sets extracted from the segmentation pipelines.

The key motivation behind incorporating comparative models was to assess the discriminative strength of handcrafted features across diverse classification architectures, ranging from linear and kernel-based methods (SVM) to tree ensembles (RF, LightGBM) and distance-based learners (KNN).

##### **Classifier Configurations**

- **SVM:** Implemented with an RBF kernel. GridSearchCV was used to tune the hyperparameters C and gamma, along with k (number of selected features). A 10-fold cross-validation strategy was employed to avoid overfitting.

- **Random Forest:** Configured with 100 decision trees and a maximum depth of 10. The model was selected for its robustness and feature importance analysis capabilities.
- **KNN:** The number of neighbors  $k$  was optimized to 7 using grid search. Euclidean distance was used as the metric, and 20 features were selected using SelectKBest.
- **LightGBM:** A gradient boosting model with shallow tree depth and regularization constraints (L1, L2) applied to reduce overfitting. Feature selection was limited to the top 30 using SelectKBest.

Each classifier was trained separately for the FCM-based and K-means-based feature sets. For consistency, SelectKBest was applied independently on the training set of each pipeline to determine the most relevant features.

Results for these models are presented in Section 3.6, along with class-wise performance comparisons against ELM.

### 3.6 Results and Discussion

This section presents the quantitative evaluation of the acne classification system across two segmentation pipelines—Fuzzy C-Means (FCM) and K-Means—and six machine learning classifiers: Extreme Learning Machine (ELM), Ensemble ELM, Support Vector Machine (SVM), Random Forest (RF), K-Nearest Neighbors (KNN), and Light Gradient Boosting Machine (LightGBM). The models were evaluated on the same dataset, using standardized preprocessing and feature extraction methods (GLCM, LBP, HSV, Gabor), with ten optimal features selected via the SelectKBest method.

#### 3.6.1 Performance on FCM-Segmented Data

The classification results on features derived from Fuzzy C-Means (FCM) segmented images are summarized in Table 4. The highest overall test accuracy of 88.00% was achieved by the Support Vector Machine (SVM) classifier, followed closely by Random Forest



(86.00%) and both the ELM and Ensemble ELM models (85.96% each). These results indicate that SVM generalized well across all three acne types, particularly pustules and nodules.

In terms of class-wise recall, ELM-based models demonstrated exceptional performance in detecting pustules (95.45%) and papules (94.74%), while their recall for nodules was lower at 62.50%, revealing challenges in distinguishing this category. KNN exhibited balanced performance with a test accuracy of 84.00%, and high recall for both nodules and papules (81.00%), indicating that proximity-based methods can be effective on structured features extracted from FCM masks.

LightGBM, however, underperformed relative to other models, with a test accuracy of 74.00%. Despite achieving perfect recall for pustules (100.00%), its recall for nodules dropped significantly to 44.00%, suggesting a tendency to overfit to more dominant class features while misclassifying underrepresented or ambiguous instances.

These findings underline the consistent difficulty across classifiers in correctly identifying nodular acne, which may be due to limited representation or feature similarity with other lesion types. Given the clinical severity associated with nodules, improving model sensitivity for this class remains an important direction for future development.

Table 3.3: Classification performance of models on FCM-segmented dataset

<b>Classifier</b>	<b>Test Accuracy (%)</b>	<b>Nodule Recall (%)</b>	<b>Papule Recall (%)</b>	<b>Pustule Recall (%)</b>
ELM	85.96	62.50	94.74	95.45
Ensemble ELM	85.96	62.50	94.74	95.45

SVM	88.00	81.00	84.00	95.00
Random Forest	86.00	81.00	79.00	95.00
KNN	84.00	81.00	79.00	91.00
LightGBM	74.00	44.00	68.00	100.00

### 3.6.2 Performance on K-Means Segmented Data

Table 5 illustrates the classification performance of the same set of models when trained on features extracted from K-Means segmented images. Compared to FCM, models under this pipeline exhibited slightly lower test accuracy overall, although performance remained relatively strong.

The ELM classifier again achieved the highest accuracy at 84.21%, followed closely by Ensemble ELM (82.46%) and KNN (81.00%). Random Forest and SVM reached 79.00% and 77.00% accuracy, respectively. These figures indicate that ELM-based classifiers maintained their effectiveness even when segmentation was performed via K-Means, showcasing their robustness to upstream variations in data representation.

Class-wise recall patterns largely mirrored those observed in the FCM pipeline. Pustules were classified with consistently high recall across all models 95.45% for both ELM variants, and 100.00% for LightGBM. The papule recall was highest in the ELM classifiers (89.47%) but declined significantly in LightGBM (53.00%) and SVM (74.00%). As in the previous pipeline, nodules remained the least accurately predicted, with recall values peaking at 62.50% for ELM and Ensemble ELM, and dropping to 44.00% for LightGBM.

The poorer performance of LightGBM in both segmentation pipelines suggests that this model may not be well-suited for datasets with relatively small size or high intra-class

variation. In contrast, ELM models consistently performed well across both pipelines, demonstrating both accuracy and stability, which are critical qualities for deployment in real-world dermatological screening applications

Table 3.4: Classification performance of models on K-means segmented dataset

<b>Classifier</b>	<b>Test Accuracy (%)</b>	<b>Nodule Recall (%)</b>	<b>Papule Recall (%)</b>	<b>Pustule Recall (%)</b>
ELM	84.21	62.50	89.47	95.45
Ensemble ELM	82.46	62.50	89.47	95.45
SVM	77.00	62.00	74.00	91.00
Random Forest	79.00	56.00	79.00	95.00
KNN	81.00	62.00	79.00	95.00
LightGBM	68.00	44.00	53.00	100.00

### 3.6.3 Comparative Discussion

A comparative evaluation of the classifiers across both segmentation pipelines reveals consistent trends in performance and highlights the impact of segmentation choice on classification outcomes. Overall, models trained on FCM-segmented data exhibited marginally superior performance compared to their counterparts trained on K-Means segmented data, particularly in terms of overall accuracy and papule recall.

Among all classifiers, the SVM trained on FCM features achieved the highest test accuracy of 88.00%, demonstrating strong generalization across all three acne classes. This was closely followed by Random Forest (86.00%), ELM (85.96%), and Ensemble ELM (85.96%) on the same pipeline. While ELM also performed strongly on the K-Means pipeline

(84.21%), the overall accuracy was slightly reduced, reaffirming that segmentation quality directly influences classification effectiveness.

In terms of per-class recall, pustules were consistently detected with high precision across all models and pipelines, often exceeding 95%, and even reaching 100% in LightGBM. This suggests that pustular lesions possess distinctive visual patterns that are well captured during feature extraction.

However, nodules emerged as the most challenging class, with recall values ranging from 44.00% to 81.00%. Notably, LightGBM exhibited the lowest nodule recall in both FCM (44.00%) and K-Means (44.00%), indicating significant model bias toward more dominant lesion types. This performance degradation may stem from the subtle morphology of nodules or their limited representation within the dataset.

Although Ensemble ELM did not surpass the top-performing classifiers in accuracy, it demonstrated stable and balanced performance across both segmentation pipelines, maintaining high recall for papules and pustules while avoiding extreme drops in nodular classification. These characteristics make it a compelling choice for deployment in real-world dermatological systems, where generalization and consistency are essential.

While LightGBM achieved perfect recall for pustules, its overall classification reliability was poor especially for nodules and papules making it unsuitable for balanced multi-class clinical applications.

Taken together, the results affirm that the choice of segmentation method substantially affects classification outcomes. The FCM pipeline, when paired with SVM or ELM-based models, provided the most accurate and balanced acne lesion classification, validating its appropriateness for this task.

A closer inspection of confusion matrix statistics for the ELM model further

underscores the superior performance of FCM-based segmentation. As shown in Table 6, the FCM pipeline produced a higher number of true positives (TP) for both papules (TP = 18) and pustules (TP = 21), along with minimal false negatives (FN = 1 for each), indicating accurate region segmentation and effective lesion localization. In contrast, the K-Means pipeline yielded lower true positives for papules (TP = 17) and a higher false positive rate (FP = 5), which reduced class-wise recall and overall reliability.

These observations are reinforced by the ROC curve analysis (see Figure 6), where the area under the curve (AUC) for the ELM model trained on FCM-segmented data was consistently higher across all classes, especially for papules and pustules, indicating improved sensitivity and specificity. The confusion matrices (Figure 5) further corroborate this, with the FCM matrix showing a stronger diagonal and fewer misclassifications than its K-Means counterpart.

This divergence in performance can be attributed to the nature of soft clustering in Fuzzy C-Means, which assigns partial membership to pixels across multiple clusters. Such flexibility captures fuzzy boundaries more accurately, especially in skin lesion images where transitions are not well-defined. In contrast, the hard-assignment nature of K-Means may lead to rigid, inaccurate masks that affect downstream feature extraction. Consequently, better segmentation in the FCM pipeline translated into more reliable features and improved classification accuracy across all classes

Table 3.5: Confusion metrics for ELM (FCM vs KMeans)

<b>Metric</b> <b>/ Class</b>	<b>Nodules</b> <b>(FCM)</b>	<b>Papules</b> <b>(FCM)</b>	<b>Pustules</b> <b>(FCM)</b>	<b>Nodules</b> <b>(KMeans)</b>	<b>Papules</b> <b>(KMeans)</b>	<b>Pustules</b> <b>(KMeans)</b>
TP	10	18	21	10	17	21

FP	1	4	3	1	5	3
FN	6	1	1	6	2	1
TN	40	34	32	40	33	32

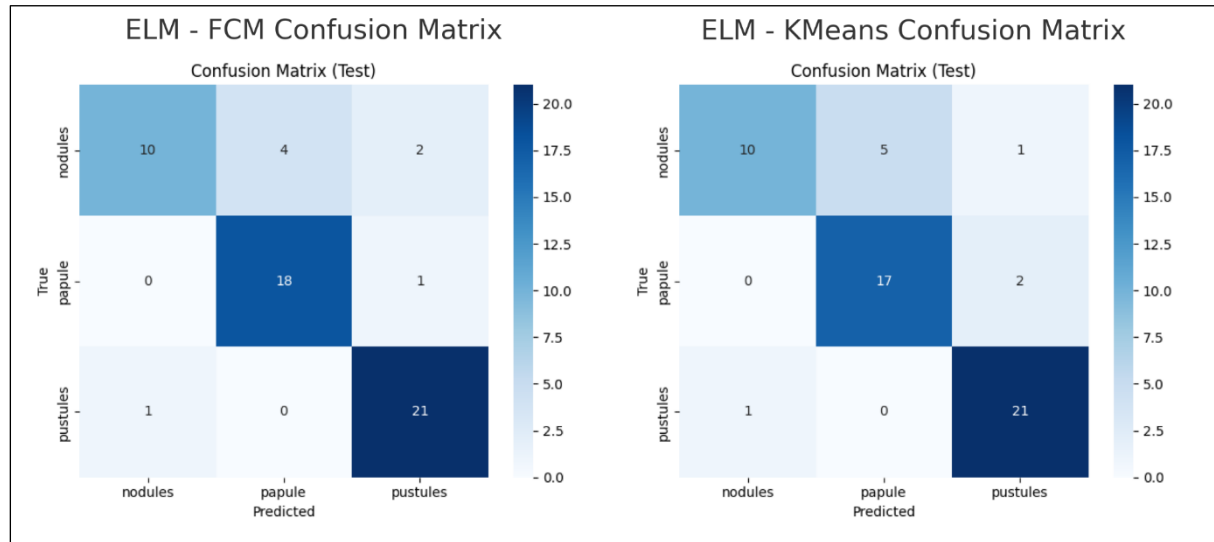


Figure 3.5: Comparison of confusion matrices for ELM classifier using FCM (left) and K-Means (right) segmentation.

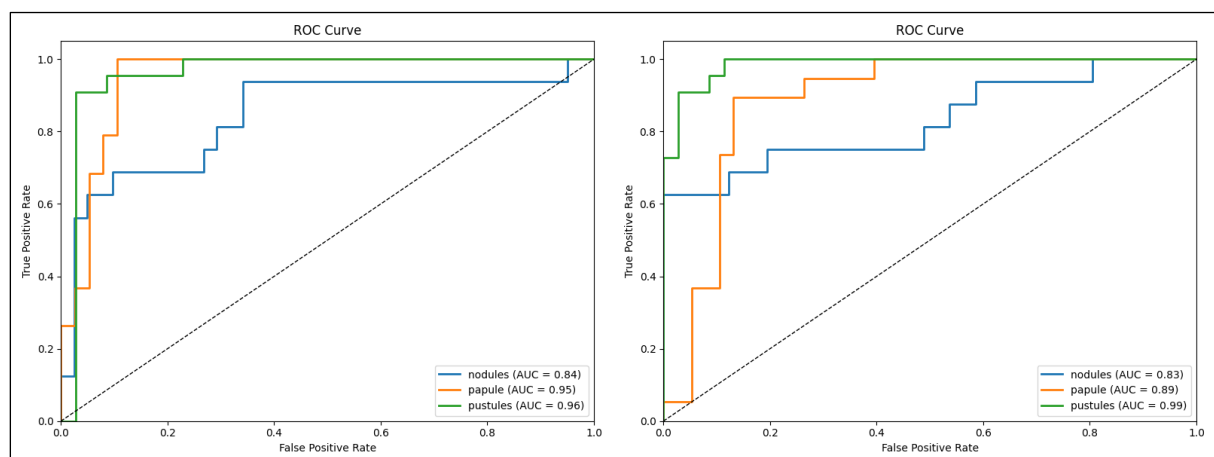


Figure 3.3: ROC curves for ELM classifier using FCM (left) and K-means (right).

## 4 CONCLUSION AND FUTURE WORK

### 4.1 Summary of Contributions

This research presented AcuCare, a lightweight, interpretable acne classification framework optimized for real-time deployment on cross-platform mobile devices. The system was designed to address key limitations in current dermatological AI systems, with a focus on unsupervised segmentation, handcrafted feature extraction, and efficient classification methods suited for resource-constrained environments.

The principal contributions of this work are summarized as follows:

- A dual segmentation pipeline employing both Fuzzy C-Means (FCM) and K-Means clustering on CLAHE-enhanced  $L^*a^*b^*$  color space images, enabling improved acne lesion isolation.
- Development of a comprehensive set of handcrafted features, incorporating texture, shape, color, and frequency-domain descriptors to effectively characterize segmented acne lesions.
- Implementation and benchmarking of multiple classifiers, notably the Extreme Learning Machine (ELM) and its ensemble variant, in comparison with established models such as Support Vector Machine (SVM), Random Forest, K-Nearest Neighbors (KNN), and LightGBM.
- Comparative analysis of segmentation pipelines, demonstrating that FCM-based features generally yielded superior classification results, especially in preserving lesion boundaries.

- Integration into a Flutter-based mobile application, capable of detecting acne, classifying lesion types, and offering over-the-counter (OTC) treatment recommendations based on the classification outcomes.

## 4.2 Key Findings

The quantitative evaluation and experimental analysis yielded several notable findings:

- Among all classifiers, SVM applied on FCM-segmented data achieved the highest classification accuracy of 88%, while the Ensemble ELM demonstrated the most consistent and balanced performance across both segmentation pipelines.
- Pustules and papules were reliably classified with high recall across all models. However, nodules posed the greatest classification challenge, attributed to their visual similarity with other lesion types and limited representation in the dataset.
- The FCM segmentation method consistently outperformed K-Means, particularly in boundary preservation and enhancing recall for less distinct lesion types.
- The mobile deployment of the system met real-world usability constraints, including low-latency inference and offline accessibility, validating its suitability for practical use.

## 4.3 Limitation

Despite its contributions, this study has several limitations:

- The dataset was relatively small (184 images in total) and exhibited slight class imbalance, with no implementation of data augmentation. This restricts the generalizability of the model to broader populations and varying skin tones.
- K-Means segmentation showed susceptibility to performance degradation under conditions of low contrast or uneven lighting, adversely affecting feature quality and subsequent classification accuracy.



- The classification model was limited to lesion type identification (nodules, papules, pustules) and did not incorporate acne severity grading, which is essential for comprehensive clinical assessment.
- The mobile application has not yet undergone clinical validation or large-scale user trials, limiting insights into its real-world reliability and user experience.

#### **4.4 Future Work**

Building upon the current findings, several directions are proposed for future research and development:

- **Dataset expansion and augmentation:** Acquiring a more diverse and balanced dataset particularly with greater representation of nodules and varied skin tones would enhance model robustness and mitigate biases.
- **Integration of severity grading:** Future versions of AcuCare could incorporate automated acne severity assessment (e.g., mild, moderate, severe), enabling more tailored treatment recommendations.
- **Hybrid segmentation strategies:** The performance of lesion isolation could be improved by integrating FCM with metaheuristic optimization algorithms such as Moth Flame Optimization (MFO) or Particle Swarm Optimization (PSO), or by exploring lightweight deep learning-based segmentation models.
- **Clinical validation and user testing:** Collaborations with dermatologists and conducting controlled user studies would provide critical feedback regarding diagnostic accuracy, usability, and patient trust.
- **Enhancing interpretability:** Implementing visual heatmaps or textual justifications for classification results could improve transparency, user trust, and adoption in clinical setting.

## 5 PROJECT DELIVERABLES

This chapter outlines the core technical and research-based outputs developed throughout the duration of the project. These deliverables encompass the mobile application, backend infrastructure, machine learning components, datasets, and documentation that collectively define the AcuCare system.

The following table summarizes the major deliverables along with brief descriptions of each

Table 5.1: Project Deliverables

Deliverable	Description
<b>AcuCare Mobile App</b>	A cross-platform mobile application developed using Flutter, designed for real-time acne detection, classification, and evidence-based treatment recommendations.
<b>Backend Classification API</b>	A Python-based Flask server hosting pre-trained classifiers, including the Ensemble Extreme Learning Machine (ELM), facilitating fast and interpretable predictions.
<b>YOLOv8-based Detection Pipeline</b>	Integration of a Roboflow-hosted YOLOv8 model for localizing acne presence in facial images prior to segmentation and classification.

<b>Dual Segmentation Pipelines</b>	Image segmentation using Fuzzy C-Means (FCM) and K-Means clustering on CLAHE-enhanced L*a*b* images to isolate acne lesions.
<b>Handcrafted Feature Extraction Module</b>	A module for computing texture (GLCM, LBP), frequency (Gabor), color, and shape-based descriptors from segmented lesion regions.
<b>Trained Machine Learning Models</b>	Pre-trained models including ELM (single and ensemble), SVM, Random Forest, KNN, and LightGBM, all saved and optimized for inference.
<b>Evaluation Framework</b>	Python scripts and visual tools for model evaluation, including classification reports, confusion matrices, and ROC curve visualizations.
<b>Custom Acne Dataset</b>	A curated dataset of 184 labeled and preprocessed acne images, annotated and structured for training and testing purposes.
<b>Thesis Document</b>	The complete academic report documenting the system architecture, methodology, experiments, and findings.
<b>Presentation Slides</b>	A formal presentation summarizing the project's objectives, methodology, technical contributions, and evaluation results.

## 6 ETHICAL CONSIDERATIONS

The development and deployment of AcuCare, an AI-based system for acne detection and treatment guidance, raise several important ethical concerns that must be carefully addressed to ensure safe and responsible usage. While the system demonstrates technical efficacy in lesion classification, its implications in a healthcare-related context necessitate a critical

evaluation of ethical principles, including user safety, fairness, transparency, and data privacy

### **6.1 Non-Diagnostic Intent**

It is imperative to emphasize that AcuCare is not intended as a diagnostic tool. The application provides automated assessments and over-the-counter treatment suggestions based on visual input; however, it does not replace clinical judgment. Users should be clearly informed that the system is designed for supportive and educational purposes only, and that professional medical consultation is essential, especially for persistent, severe, or atypical acne conditions.

### **6.2 Bias and Generalizability**

The dataset used for training the classification models comprises 184 labeled acne images, which may not comprehensively represent the full spectrum of skin tones, ethnicities, and lesion types. This poses a risk of algorithmic bias, where the model may underperform on underrepresented groups. Such bias can lead to misclassification, reduced trust, and potential harm if not properly disclosed. Future efforts should focus on dataset diversification and fairness-aware training strategies to improve model generalizability and inclusivity.

### **6.3 Privacy and Data Handling**

As the system processes sensitive facial imagery, stringent attention must be given to user privacy and data protection. While the current prototype may not store images, any production-level deployment must incorporate secure storage protocols, encryption mechanisms, and on-device inference wherever possible to minimize exposure risks. Additionally, compliance with relevant data protection regulations (e.g., GDPR, HIPAA) should be ensured, depending on the deployment context.

### **6.4 Informed Usage**

Users must be provided with clear disclaimers and educational content regarding the

capabilities and limitations of the AI system. This includes:

- Transparency about the system's accuracy levels and non-clinical status.
- Guidance on when to seek professional help.
- An overview of how user data is processed and protected.

Such measures promote informed consent and empower users to interpret results critically rather than blindly trusting algorithmic outputs.

## **6.5 Responsibility and Future Development**

To ensure ethical integrity and societal value, future iterations of AcuCare should prioritize:

- Clinical validation through collaboration with dermatologists and user studies.
- Explainable AI techniques that provide interpretable outputs or visual justifications.
- Fairness-aware design to mitigate biases across demographic groups.
- Continuous feedback mechanisms to improve system performance and user experience over time.

## REFERENCES

- [1] G. Schaefer, M. I. Rajab, M. E. Celebi, and H. Iyatomi, "Colour and contrast enhancement for improved skin lesion segmentation.," *Comput Med Imaging Graph*, vol. 35, no. 2, pp. 99–104, Mar. 2011, doi: [10.1016/j.compmedimag.2010.08.004](https://doi.org/10.1016/j.compmedimag.2010.08.004).
- [2] Ç. Suiçmez, H. T. Kahraman, A. Suiçmez, C. Yılmaz, and F. Balcı, "Detection of melanoma with hybrid learning method by removing hair from dermoscopic images using image processing techniques and wavelet transform," *Biomedical Signal Processing and Control*, vol. 84, p. 104729, 2023, doi: <https://doi.org/10.1016/j.bspc.2023.104729>.
- [3] J. Khan, A. Malik, N. Kamel, S. Das, and A. Mohd Affandi, *Effect of color feature normalization on segmentation of color images*. 2016, p. 5. doi: [10.1109/ICIAS.2016.7824099](https://doi.org/10.1109/ICIAS.2016.7824099).
- [4] H. Zhang and T. Ma, "Acne Detection by Ensemble Neural Networks.," *Sensors (Basel)*, vol. 22, no. 18, Sep. 2022, doi: [10.3390/s22186828](https://doi.org/10.3390/s22186828).
- [5] X. Wu *et al.*, "Joint Acne Image Grading and Counting via Label Distribution Learning," *2019 IEEE/CVF International Conference on Computer Vision (ICCV)*, Seoul, Korea (South), 2019, pp. 10641-10650, doi: [10.1109/ICCV.2019.01074](https://doi.org/10.1109/ICCV.2019.01074).
- [6] M. Moncho-Santonja, S. Aparisi-Navarro, B. Defez, and G. Peris-Fajarnés, "Segmentation of Acne Vulgaris Images Techniques: A Comparative and Technical Study," *Applied Sciences*, vol. 13, no. 10, 2023, doi: [10.3390/app13106157](https://doi.org/10.3390/app13106157).
- [7] M. S. Junayed *et al.*, "AcneNet - A Deep CNN Based Classification Approach for Acne Classes," *2019 12th International Conference on Information & Communication*

*Technology and System (ICTS)*, Surabaya, Indonesia, 2019, pp. 203-208, doi: 10.1109/ICTS.2019.8850935.

[8] S. Garg and B. Jindal, "Skin lesion segmentation using k-mean and optimized fire fly algorithm," *Multimedia Tools and Applications*, vol. 80, pp. 1–14, Feb. 2021, doi: [10.1007/s11042-020-10064-8](https://doi.org/10.1007/s11042-020-10064-8).

[9] A. S. Buriboev, A. Khashimov, A. Abduvaitov, and H. S. Jeon, "CNN-Based Kidney Segmentation Using a Modified CLAHE Algorithm," *Sensors*, vol. 24, no. 23, 2024, doi: [10.3390/s24237703](https://doi.org/10.3390/s24237703).

[10] M. A. M. Almeida and I. A. X. Santos, "Classification Models for Skin Tumor Detection Using Texture Analysis in Medical Images," *Journal of Imaging*, vol. 6, no. 6, 2020, doi: [10.3390/jimaging6060051](https://doi.org/10.3390/jimaging6060051).

[11] N. Gao *et al.*, "Evaluation of an acne lesion detection and severity grading model for Chinese population in online and offline healthcare scenarios," *Scientific Reports*, vol. 15, no. 1, p. 1119, Jan. 2025, doi: [10.1038/s41598-024-84670-z](https://doi.org/10.1038/s41598-024-84670-z).

[12] I. R. Rodrigues, S. R. da Silva Neto, J. Kelner, D. Sadok, and P. T. Endo, "Convolutional Extreme Learning Machines: A Systematic Review," *Informatics*, vol. 8, no. 2, 2021, doi: [10.3390/informatics8020033](https://doi.org/10.3390/informatics8020033).

[13] N. Kittigul and B. Uyyanonvara, "Acne Detection Using Speeded up Robust Features and Quantification Using K-Nearest Neighbors Algorithm," *Proceedings of the 6th International Conference on Bioinformatics and Biomedical Science*, 2017, [Online]. Available: <https://api.semanticscholar.org/CorpusID:21525581>.

[14] S. Lucut and M. R. Smith, "Dermatological tracking of chronic acne treatment effectiveness," *2016 38th Annual International Conference of the IEEE Engineering in*

*Medicine and Biology Society (EMBC)*, Orlando, FL, USA, 2016, pp. 5421-5426, doi: 10.1109/EMBC.2016.7591953.

[15] R. Latifahul Hasanah, Y. Rianto, and D. Riana, "Identification of Acne Vulgaris Type in Facial Acne Images Using GLCM Feature Extraction and Extreme Learning Machine Algorithm," *Rekayasa*, vol. 15, pp. 204–214, Aug. 2022, doi: [10.21107/rekayasa.v15i2.14580](https://doi.org/10.21107/rekayasa.v15i2.14580).

[16] R. Ramli, A. S. Malik, A. F. M. Hani, and F. B.-B. Yap, "Identification of acne lesions, scars and normal skin for acne vulgaris cases," *2011 National Postgraduate Conference*, pp. 1–4, 2011.

[17] N. Alamdari, K. Tavakolian, M. Alhashim, and R. Fazel-Rezai, "Detection and classification of acne lesions in acne patients: A mobile application," *2016 IEEE International Conference on Electro Information Technology (EIT)*, pp. 0739–0743, 2016.



## APPENDIX

### Appendix A: Flowchart

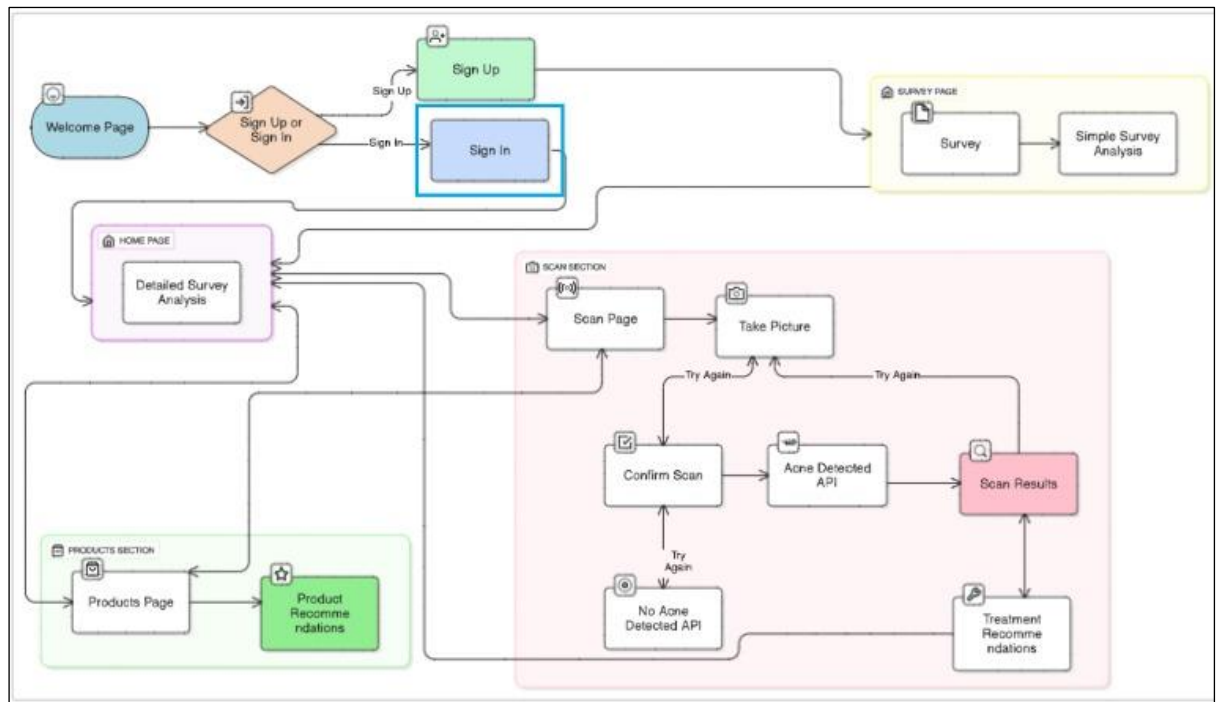


Figure A 1: Flowchart of the working of mobile application

## Appendix B: Use case Diagram

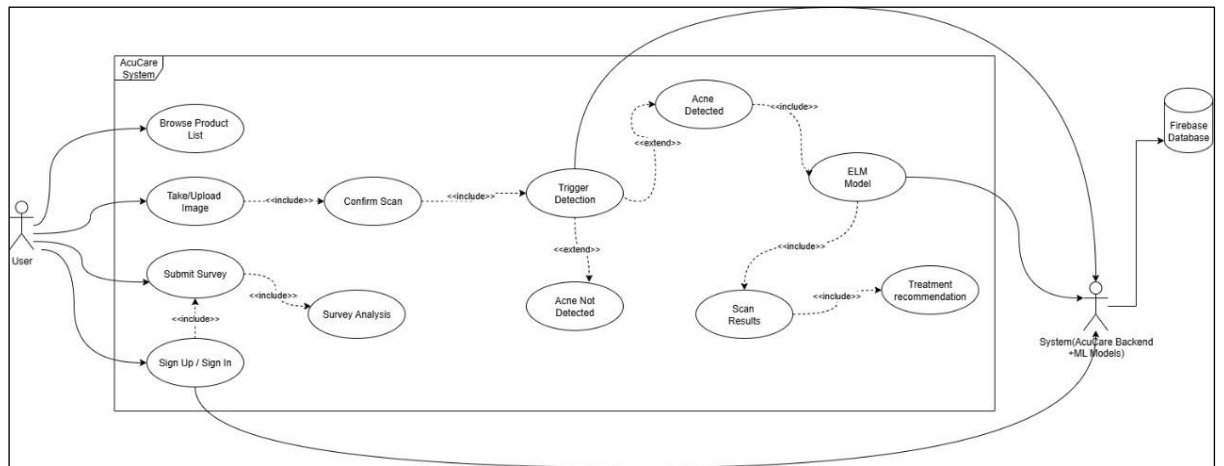


Figure A 2: Use Case Diagram.

